Congenital Zika Syndrome is associated with maternal genetic background

Authors

Tamiris Azamor[1,2], Daniela Prado Cunha[3], Andréa Marques Vieira da Silva[2], Ohanna Cavalcanti de Lima Bezerra[1], Marcelo Ribeiro-Alves[4], Thyago Leal Calvo[1], Fernanda de Souza Gomes Kehdy [1], Fernanda Saloum de Neves Manta[1], Thyago Gomes Pinto[1], Laís Pereira Ferreira[1], Elyzabeth Avvad Portari[3], Letícia da Cunha Guida[3], Leonardo Gomes[3], Maria Elisabeth Lopes Moreira[3], Elizeu de Carvalho[5], Cynthia Chester Cardoso[6], Marcelo Muller[2], Patrícia Cristina da Costa Neves[2], Zilton Vasconcelos[3], Milton Ozorio Moraes[1]*

1 Laboratório de Hanseníase. Instituto Oswaldo Cruz. Fiocruz, Brazil.
2 Vice-Diretoria de Desenvolvimento Tecnológico. Instituto de Tecnologia em Imunobiológicos, Fiocruz, Brazil.
3 Unidade de Pesquisa Clínica, Instituto Nacional de Saúde da Mulher, da Criança e do Adolescente Fernandes Figueira. Fiocruz, Brazil.
4 Laboratório de Pesquisa Clínica em DST/AIDS. Instituto Nacional de Infectologia. Fiocruz, Brazil.
5 Laboratório de Diagnóstico por DNA. Universidade do Estado do Rio de Janeiro, Brazil.
6 Laboratório de Virologia Molecular. Universidade Federal do Rio de Janeiro, Brazil.

*Correspondence: milton.moraes@fiocruz.br

Graphical abstract

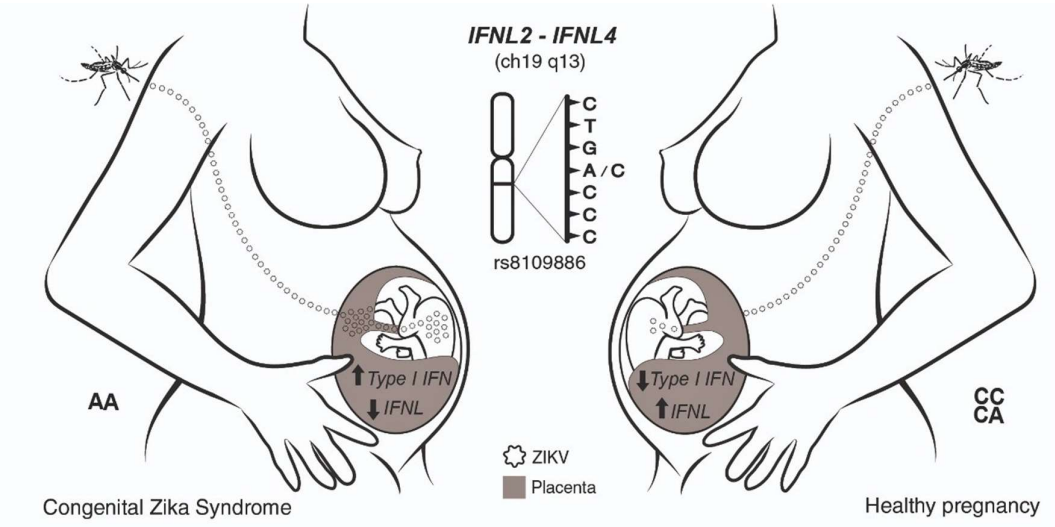

Summary

Maternal and/or fetal factors that influence Congenital Zika Syndrome (CZS) development remain elusive. Interferon lambda has been reported as an antiviral factor in Zika infections. Using functional analysis, we conducted a case-control study to demonstrate that maternal interferon lambda single nucleotide polymorphisms (SNPs) contribute to newborn protection. Mothers carrying CA/CC genotypes of rs8109886 SNP have 4.5 times reduced risk of having children with CZS. When we combined the genotypes CC from rs12979860 and CA/CC from rs8109886, 93% of the mothers delivered healthy newborns. Placenta coming from CZS cases displayed diminished level of *IFNL2* along with higher tissue-specific type-I IFN genes, tagged by of *IFIT5*, indicating that lower *IFNL* levels upon ZIKV infection can lead to uncontrolled damage to overexpression of type-I IFN pathway. In summary, genetically regulated *IFNL* levels contribute to immune homeostasis and CZS prevention.

Key words: Congenital Zika Syndrome, Interferon lambda, SNPs.

INTRODUCTION

Zika virus (ZIKV) is a single strand positive-sense RNA virus that belongs to the Flaviviridae family; this infection is mostly asymptomatic or associated with mild symptoms. After the outbreak in the Americas in 2015, the virus spread across 59 countries and more than 500.000 suspected cases were reported (Relich and Loeffelholz, 2017). In a short while, there was a rise in the cases of congenital abnormalities, including cerebral anomalies, congenital contractures, and ocular alterations besides neurological abnormalities known as Congenital Zika Syndrome (CZS) (Adhikari et al., 2017; de Araújo et al., 2018; Jürgens and Rey, 2018; Wen et al., 2017). In a prospective cohort study, our group observed that 46% of the infants that were born to ZIKV-infected mothers bore abnormal clinical or brain imaging findings, including four infants with microcephaly, regardless of the trimester in pregnancy (Brasil et al., 2016) . Indeed, in a little while, and a case-control study confirmed the association between the infection and CZS and ZIKV epidemic was declared a public health emergence of international concern (de Araújo et al., 2018; 2017b). Nevertheless, not all the infants that are born to ZIKV- infected mothers will develop CZS, and it is not clear what maternal and/or fetal factors contribute to infant adverse neurologic outcomes. One important risk factor for CSZ is infection within the first trimester of pregnancy, which poses almost twice as high risks of severe outcomes as CNS abnormalities when compared with the third trimester infections (Brasil et al., 2016). It has been reported that genetic

background can influence the outcome, although no targets or candidates have been identified, and it is likely that mothers' genetic factors could also be involved in CZS outcome (Caires-Júnior et al., 2018).

During other congenital infections, namely TORCH (Toxoplasma, Others, Rubella, Cytomegalovirus, Herpes), which may cause malformations, placenta has been described as playing a crucial role in mother to fetus transmissions (Coyne and Lazear, 2016). In ZIKV infection, one of the hypotheses for the emergence of adverse neurological outcomes is that ZIKV can infect and cross trophoblast cell layers as a cargo to reach the fetal neurologic system, causing direct damage. On the other hand, ZIKV infection would cause an immunological imbalance in the placenta, disrupting the embryonic brain development (Bayer et al., 2016; Delorme-Axford et al., 2013; Grant et al., 2016; Hirsch et al., 2018; Noronha et al., 2016; Quicke et al., 2016; Tabata et al., 2016). This theory is aligned with other situations where microcephaly may occur, such as radiation exposure, tobacco smoke, cocaine use, alcohol consumption, cytomegalovirus, or α-hemolytic streptococci infections (Dekaban, 1968; Hadeed and Siegel, 1989; Leviton et al., 2010; Mostoufi-zadeh et al., 1984).

Type III interferons (a.k.a. IFN-λ 1-4) are key antiviral molecules that present an augmented expression during the ZIKV infection in susceptible placental cells(Bayer et al., 2016). Despite chimeric maternal-fetal properties of placenta, only the maternal component exhibit type III interferon response after ZIKV infection (Weisblum et al., 2017). Further, single nucleotide polymorphisms (SNPs) in these genes regulate the *IFNL1-4* expression and are associated with the outcome of the infectious diseases(O'Brien et al., 2014). Notably, SNPs in the vicinity of IFN-λ4 are associated with HCV clearance—another member of Flaviviridae family (Suppiah et al., 2009). Interestingly, the effects of rs12979860 CC genotype have been observed in postpartum normal pregnancy, associated with persistent low level of ISGs *IFIT1*, *IFIT2*, *IFIT3*, and *OAS1*(Price et al., 2016).

In this paper, we describe the association between the genetic background of ZIKV-infected pregnancy and CZS development, focusing on the SNPs located in the region spanning *IFNL2* to *IFNL4* genes, as well as the functional consequences of specific genotypes for the immunological imbalance in placenta.

RESULTS

Maternal CA/CC genotype of SNP rs8109886 is a protective factor against CZS outcome

We used principal component analysis to retrieve 320 SNPs located in the *IFNL* region which are found among the African and European populations from 1000 Genomes Project (Figure S1A); we selected four representative SNPs (rs12979860, rs4803222, rs8109886, and rs8099917) to construct the haplotypes in parental populations. The allele frequencies, annotation, and reference of the selected SNPs are described in Table S1. The linkage disequilibrium (LD) analysis indicated that, in contrast to the Africans (r2=0.17), SNPs rs12979860 and rs4803222 were in strong LD among the Europeans from 1000 Genomes population (r2 = 0.90) (Figure S1B). The arranged haplotypes, tagged by rs12979860 and rs8109886 alleles, have very different frequencies among the Africans and Europeans (Table S2).

The DNA samples from whole blood of 92 ZIKV-infected women, with development of CZS (cases) or otherwise (controls), were genotyped for the SNPs encompassing *IFNL4* gene (rs12979860 and rs4803222) and between *IFNL2* and *IFNL4* genes (rs8099917 and rs8109886). The frequency of each SNP was verified in cases and controls, and the CZS outcome was evaluated. In all the SNPs tested, the genotype frequencies were found in HWE except rs8099917. The data were then adjusted by the trimester of pregnancy— when the symptoms of ZIKV infection were detected—and ancestry (based on genotyping a panel of 46 ancestry informative markers), since we observed differences in haplotype frequencies among the Africans and Europeans (Table S2). A statistically significant protection was found for the C allele carriers of SNP rs8109886 (OR = 0.22; CI = 0.05–0.91, p = 0.028) (Table 1). No differences were observed in the frequencies between cases and controls in any other SNPs tested. Since rs12979860 is classically associated with HCV clearance upon IFNα treatment and tag high frequency haplotypes among the Africans and Europeans, we decided to include it in the analysis. Data indicate that an arrangement of rs8109886 C-rs12979860 C is present in 39% of no CZS, whereas only 1.9% has abnormal CZS (OR = 0.07; CI=0.01–0.5, p = 0.003 after co-variate adjustments) (Table S3). The clusterization according genotype combination show that CC/CA- CC (rs8109886-rs12979860) combinations resulted in 93% of 'No CZS' cases, (Figure 1), while combinations carrying the rs8109886AA genotypes were more frequent among the mothers with CZS children. All the other genotypic analyses included children genotypes or mother:children pairs did not show any significant results (Tables S4 and S5).

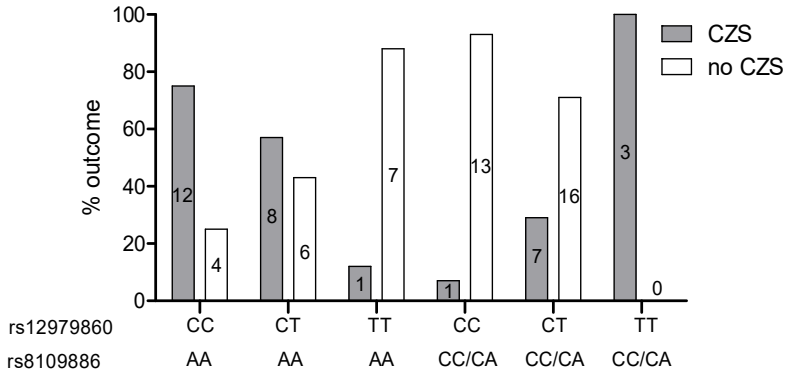

Figure 1. Percentage of CSZ or no CZS outcomes, clustered by genotypic combinations between rs8109886 and rs12979860. The values within the bars represent the absolute number of cases. The total number of the genotyped combinations may vary due to genotype miscalling for each SNP.

Table 1. Association with mother *IFNL*2-*IFNL*4 SNPs and CZS abnormalities

	No CZS findings		Abnormal CZS		No adjustment			Adjusted by trimester of exposure to ZIKV			Adjusted by trimester of exposure to ZIKV and ancestrality		
	N[a]	(%)	N[a]	(%)	OR	CI (95%)	p-value	OR	CI (95%)	p-value	OR	CI (95%)	p-value
						rs8109886							
AA	17	37.0	22	66.7	Ref		0.031*	ref		0.025*	ref		0.087
CA	23	50.0	9	27.3	0.30	0.11-0.82		0.20	0.06-0.75		0.21	0.05-0.93	
CC	6	13.0	2	6.1	0.26	0.05-1.44		0.22	0.03-1.52		0.29	0.03-2.82	
AA	17	37.0	22	66.7	Ref		0.008***	ref		0.006***	ref		0.028*
CC/CA	29	63.0	11	33.3	0.29	0.11-0.75		0.21	0.06-0.68		0.22	0.05-0.91	
AA/CA	40	87.0	31	93.9	Ref		0.296	ref		0.329	ref		0.666
CC	6	13.0	2	6.1	0.43	0.08-2.28		0.42	0.07-2.62		0.63	0.08-5.31	
AA/CC	23	50.0	24	72.7	Ref		0.040*	ref		0.029*	ref		0.057
AC	23	50.0	9	27.3	0.38	0.14-0.98		0.27	0.08-0.92		0.27	0.07-1.11	
Additive	46	58.2	33	41.8	0.40	0.19-0.86	0.012*	0.35	0.14-0.85	0.014*	0.37	0.13-1.12	0.063
						rs8099917							
TT	31	67.4	24	72.7	Ref		0.481	ref		0.229	ref		0.236
GT	14	30.4	7	21.2	0.65	0.23-1.85		0.35	0.09-1.41		0.30	0.60-1.46	
GG	1	2.2	2	6.1	2.58	0.22-30.2		2.62	0.09-74.9		1.94	0.08-47.01	
TT	31	67.4	24	72.7	Ref		0.6099	ref		0.217	ref		0.199
GG/GT	15	32.6	9	27.3	0.78	0.29-2.07		0.46	0.13-1.64		0.40	0.09-1.71	
TT/GT	45	97.8	31	93.9	Ref		0.3758	ref		0.454	ref		0.519
GG	1	2.2	2	6.1	2.90	0.25-33.4		3.32	0.13-87.1		2.72	0.12-60.5	
TT/GG	32	69.6	26	78.8	Ref		0.375	ref		0.106	ref		0.099
GT	14	30.4	7	21.2	0.62	0.22-1.75		0.33	0.08-1.34		0.28	0.06-1.38	
Additive	46	58.2	33	41.8	0.95	0.42-2.16	0.9077	0.67	0.24-1.85	0.441	0.63	0.20-1.98	0.418
						rs12979860							
CC	20	40.8	20	47.6	Ref		0.708	ref		0.787	ref		0.964
CT	22	44.9	18	42.9	0.82	0.34-1.97		0.72	0.25-2.08		0.94	0.29-3.08	
TT	7	14.3	4	9.5	0.57	0.14-2.26		0.67	0.15-3.09		0.80	0.15-4.16	
CC	20	40.8	20	47.6	Ref		0.514	ref		0.492	ref		0.856
TT/CT	29	59.2	22	52.4	0.76	0.33-1.74		0.71	0.26-1.90		0.90	0.29-2.77	
CC/CT	42	85.7	38	90.5	Ref		0.4840	ref		0.743	ref		0.803
TT	7	14.3	4	9.5	0.63	0.17-2.33		0.79	0.19-3.32		0.83	0.18-3.76	
CC/TT	27	55.1	24	57.1	Ref		0.8449	ref		0.642	ref		0.996
CT	22	44.9	18	42.9	0.92	0.92-0.40		0.79	0.29-2.15		1.00	0.34-2.98	
Additive	49	53.8	42	46.2	0.78	0.42-1.43	0.4157	0.79	0.39-1.61	0.390	0.90	0.41-1.98	0.798
						rs4803222							
GG	22	45.8	20	55.6	Ref		0.361	ref		0.252	ref		0.236
CG	23	47.9	12	33.3	0.57	0.23-1.45		0.48	0.14-1.57		0.42	0.10-1.75	
CC	3	6.2	4	11.1	1.47	0.29-7.37		2.25	0.28-17.8		2.69	0.26-28.14	
GG	22	45.8	20	55.6	Ref		0.377	ref		0.419	ref		0.426
CG/CC	26	54.2	16	44.4	0.68	0.28-1.61		0.64	0.21-1.91		0.59	0.16-2.18	
GG/CG	45	93.8	32	88.9	Ref		0.427	ref		0.2681	ref		0.236
CC	3	6.2	4	11.1	1.87	0.39-8.96		3.07	0.41-23.5		3.98	0.41-39.1	
GG/CC	25	52.1	24	66.7	Ref		0.177	ref		0.1430	ref		0.137
CG	23	47.9	12	33.3	0.54	0.22-1.33		0.43	0.13-1.36		0.36	0.09-1.44	
Additive	48	57.1	36	42.9	0.89	0.45-1.75	0.730	0.94	0.40-2.18	0.8813	0.95	0.34-2.63	0.913

DNA samples from 92 mothers with congenital infection by ZIKV, with developed CZS or not, were genotyped for rs12979860, rs8109886, rs8099917, and rs4803222 SNPs at *IFNL*2 and *IFNL*4. Data were adjusted considering the trimester of the first symptoms or asymptomatic ZIKV infections and the percentage of the African and European ancestry of each individual[a]. The total number of the genotyped samples for each SNP may vary due to genotype miscalling. Major allele was used as baseline. Odds ratio (OR) with 95% confidence interval (CI) and p-values.

Congenital ZIKV infection leads to an immunological imbalance in placenta

To verify functionally how *IFNL* genotypes would influence ZIKV severe congenital outcomes we performed gene expression analyses from the chimeric fetal-maternal placental tissues, obtained the time of delivery from 10 uninfected pregnant woman and 74 congenital ZIKV cases (Table S6). We used a multiplex RT-qPCR analysis of 96 candidate genes, selected based on innate and antiviral immunity and only statistically significant results are presented. First, all the RT-PCR ZIKV positive samples at term showed higher gene expression in most genes analyzed. ZIKV congenital infections occurring at the third trimester of pregnancy resulted in higher gene expression levels. The advanced maternal age mothers expressed lower levels of inflammatory genes, suggesting natural immunological senescence (Table S7). Because of these intrinsic differential expression profile, ZIKV RT-qPCR positive placenta, trimester of exposure to ZIKV, and mothers age greater than or equal to 40 years were considered as confounding variables in gene expression analysis of congenital ZIKV cases.

We observed that placental gene expression from congenital ZIKV infections exhibited an increased expression of *IFIT5*, *IFNA1*, *IFNB*, *IFI16*, *IL22RA*, *IP10*, *IRF7*, and *IRF9*, and a decreased expression of *TYRO3*, when compared with uninfected pregnant women (Figure 2). This result indicates that ZIKV infection leads to a typical inflammatory response in the placenta, including the expression of anti-viral Type I interferon genes (*IFIT5*, *IFNA1*, and *IFNB*), Type II interferon (*IFI16*), cytokine signaling (*IL22RA* and *IP10*), and interferon regulatory factors (*IRF7* and *IRF9*).

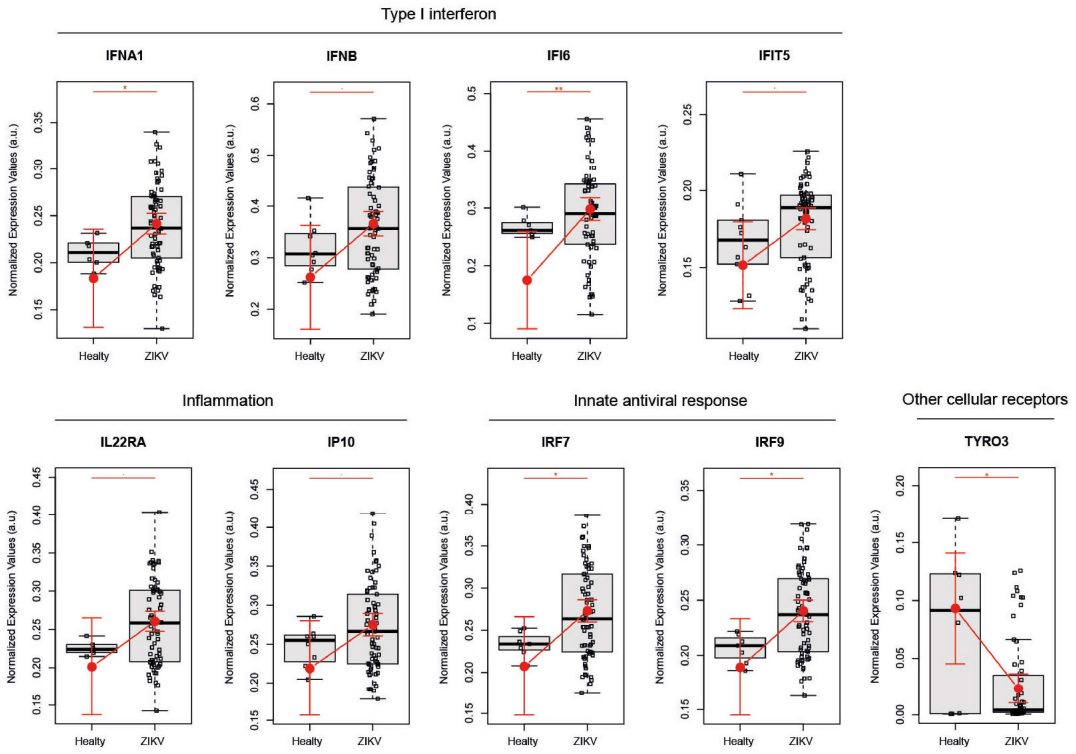

Figure 2. ZIKV infection leads to an immunological imbalance in placenta. Placental gene expression profile in healthy (N = 10) versus ZIKV-infected women (N = 74). Each point corresponds to one placenta analyzed. The number of dots varies according to gene analyzed due to failed amplifications. The median and standard deviation of gene expression values are normalized by the housekeeping genes, selected by the geNorm and NormFinder as well as *18S* ribosomal RNA and *RLP13* ribosomal protein L13 (grey boxes); values are adjusted by mothers' age (below or equal to/above 40 years old) and infection trimester (the trimester of pregnancy which occurs first Zika symptoms or asymptomatic ZIKV infections) (red lines). Pairwise comparisons of log-transformed (base 2) normalized expression means between/among the groups of interest were performed by contrasts/differences (fold-changes), obtained after both bi- and multivariate linear models modified by ordinary least square regressions. Whenever the variable of interest had more than two levels, p-values were corrected by the Tukey Honest Significant Difference post-Hoc method. After all the gene-per-gene pairwise comparisons were made, we conducted a Type I error adjustment for the multiple comparisons following the Holm-Bonferroni method. P-values ** ≤ 0.01, * ≤ 0.05 and ≤ 0.1.

Interestingly, ZIKV PCR+ placentas showed an increased expression in several Type III interferons as well as Type I interferon genes analyzed, except for *IFITM1*, which presented reduced expression. Data also demonstrated an augmented expression of *CLEC5A* and *DCSIGN* as well as *TLR3* and *TLR8* (pattern- recognition) receptors, *BCL2*, *CARD9* (apoptosis-related), *IL18* and *AIM2* (Type II interferon) and *IFNL1* (Type III interferon). Corroborating the ZIKV-infection pro- inflammatory placental profile, results showed an elevated expression of chemokine- related genes (i.e., *CCR2*, *CCR3*, *CCR5*, *MIP1A*, and *IP10*) and other cytokine-related genes (i.e., *IL22A*, *MMP2*, and *TNF*) besides *NRPL3*, which

denotes the presence of inflammasome activation in placenta with ZIKV PCR+ samples. Results also showed an increase in the expression of *IL10* (Figure S2).

Decreased *IFNL2* in placenta at term is associated with newborn CNS abnormalities

Next, we tested whether the gene expression signatures of placentas coming from ZIKV-infected women could be associated with the presence or absence of abnormal Central Nervous System (CNS) formation. These analyses illustrated *IFNL2* and *ISG15* significant decreases in newborns with CNS alterations, demonstrating that a sustained Type-III IFN genes activation may be required to prevent abnormal CZS. On the other hand, *IFIT5* showed a significant increase in newborns with CNS abnormalities group, and given that the results with PCR-positive ZIKV placenta also show increased levels of *IFIT5*, these data suggest a persistent infection that could be associated with more severe outcomes (Figure 3).

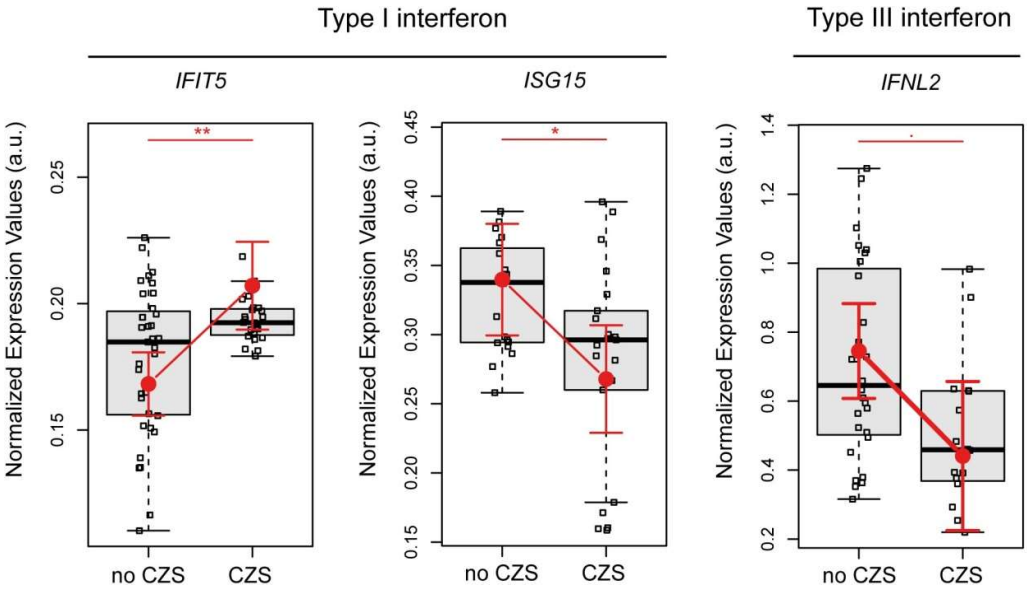

Figure 3. Placental gene expression associated with CZS. Detailed graphics of differentially expressed genes in placenta without CZS (No CZS; N = 45) or with abnormal CZS (CZS; N = 29). Each point corresponds to one placenta analyzed. The number of dots varies according to gene analyzed due to failed amplifications. The median and standard deviation of gene expression values are normalized by the housekeeping genes, selected by the geNorm and NormFinder as well as *18S* ribosomal RNA and *RLP13* ribosomal protein L13 (grey boxes); values are adjusted by mothers' age (below or equal to/above 40 years old) and infection trimester (the trimester of pregnancy which occurs first Zika symptoms or asymptomatic ZIKV infections) (red lines). Pairwise comparisons of log- transformed (base 2) normalized expression means between/among the groups of interest were performed by contrasts/differences (fold-changes), obtained after both bi- and multivariate linear models modified by ordinary least square regressions. Whenever the variable of interest had more than two levels, p-values were corrected by the Tukey Honest Significant Difference post-Hoc method. After all the gene-per-gene pairwise comparisons were made, we conducted a Type I error adjustment for the multiple comparisons following the Holm-Bonferroni method. P-values ** ≤ 0.01, * ≤ 0.05, and ≤ 0.1.

Rs8109886 genotypes CA/CC in mothers are associated with balanced placental *IFIT5* and elevated *IFNL3/4* expression

We accessed 30 DNA samples from mothers that had the placenta analyzed, thus placenta gene expression was clustered according to different genotypes (i.e., CA/CC and AA) to validate the case-control analysis of rs8109886. Our data showed that placentas coming from rs8109886 AA mothers showed a significantly increased expression of *IFIT5*, *IFNA1*, *IL2*, *MIP1B*, *MMP2*, *IL10*, *IRF7*, *IRF9*, and *OAS3* (Figure S3). This result suggests that rs8109886 AA mothers have an exacerbated and uncontrolled cytokine profile, compared with CA/CC mothers. Next, we verified whether placental gene expression in abnormal CZS or no CZS could be modulated by rs8109886 CA/CC and AA genotype. Data show that CA/CC mothers have a low expression of Type-I IFN ISG *IFIT5* and *MMP9* besides a visible high expression of *IFNL3/4* (Figure 4A). Together, these data demonstrate that rs8109886 could act as a modulator for both Type-I IFN and *IFNL*; mothers with CA/CC genotypes can achieve a balanced response between these two mediators, which are essential to a healthy pregnancy (Figure 4B).

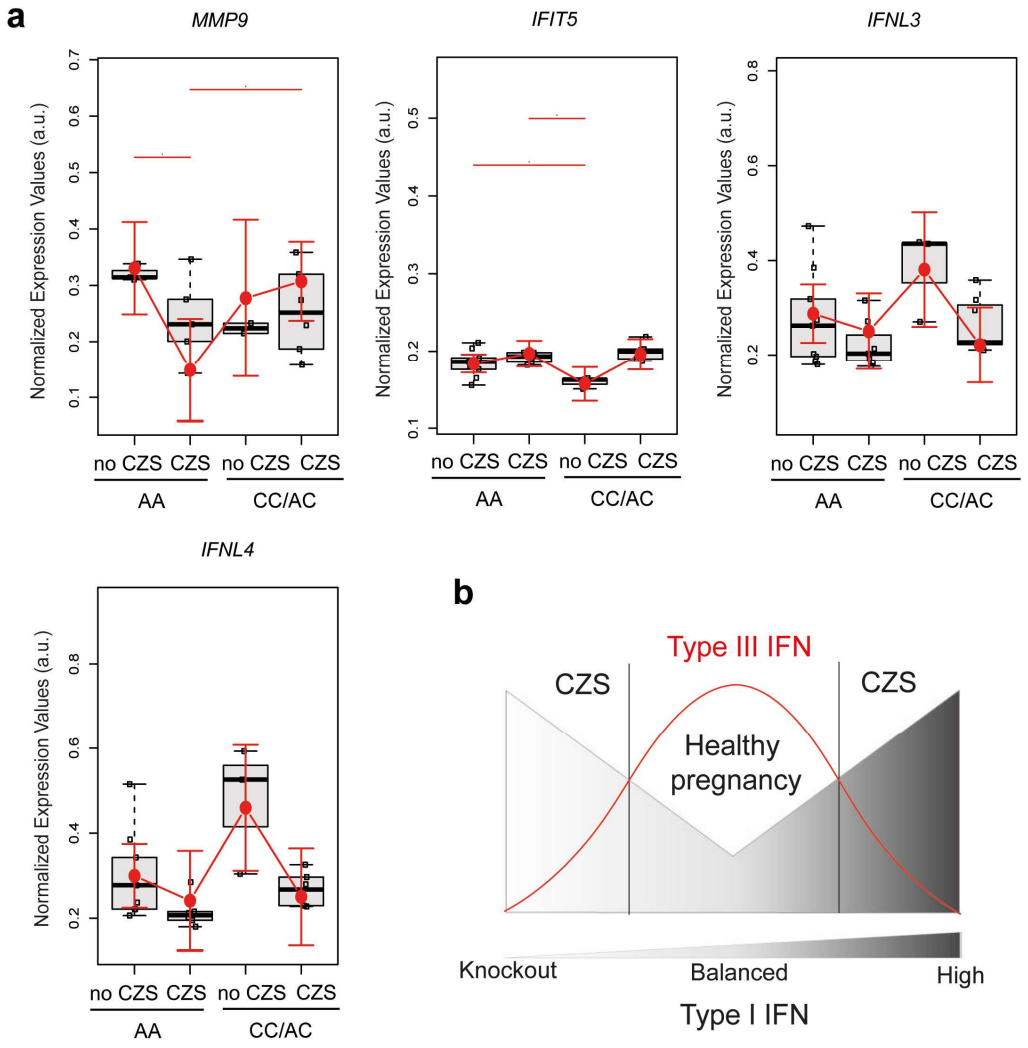

Figure 4. Placental gene expression associated with CZS is modulated by rs8109886 genotype. (a) Detailed graphics of differentially expressed genes in placenta from no CZS rs8109886 AA (N = 10) or CA/CC mothers (N = 4) and CZS AA (N = 9) or CA/CC mothers (N = 7). Each point corresponds to one placenta analyzed. The number of dots varies according to gene analyzed due to failed amplifications. The median and standard deviation of gene expression values are normalized by the housekeeping genes, selected by the geNorm and NormFinder as well as *18S* ribosomal RNA and *RLP13* ribosomal protein L13 (grey boxes); values are adjusted by mothers' age (below or equal to/above 40 years old) and infection trimester (the trimester of pregnancy which occurs first Zika symptoms or asymptomatic ZIKV infections) (red lines). Pairwise comparisons of log-transformed (base 2) normalized expression means between/among the groups of interest were performed by contrasts/differences (fold-changes), obtained after both bi- and multivariate linear models modified by ordinary least square regressions. Whenever the variable of interest had more than two levels, p-values were corrected by the Tukey Honest Significant Difference post-Hoc method. After all the gene-per-gene pairwise comparisons were made, we conducted a Type I error adjustment for the multiple comparisons following the Holm-Bonferroni method. P-values **≤ 0.01, * ≤ 0.05, and ≤ 0.1. (c) Schematic representation of the relation between Type I and III IFN in congenital ZIKV infections regarding abnormal CZS, showing that lower risk of developing CZS is related to higher levels of IFNL and balanced levels of Type-I IFN.

DISCUSSION

Despite the high risk, ZIKV infection during pregnancy is necessary, albeit not sufficient, to induce CZS. Here, we conducted a case-control study with CZS cases and healthy ZIKV^{+} mothers. We hypothesized that host genetic background, especially *IFNL* SNPs, could contribute to CSZ development. *IFNL* SNPs were described as central in the therapeutic responses to another chronic flavivirus pathogen, Hepatitis C, which is probably one of the most important genetic findings of GWAS era(Bayer et al., 2016; Price et al., 2006; Suppiah et al., 2009; Tanaka et al., 2009). Specifically, our results demonstrated that mothers who carried the CA/CC genotypes of SNP rs8109886 (*IFNL2-IFNL4*) had a 4.5 reduced risk (OR = 0.22) of having children with abnormal CZS, resulting from congenital ZIKV infection, compared with those with AA genotype. One important issue was that ancestry tends to have impacted on the distribution of the major haplotypes studied here; this was done in such a way that we included a panel of AIMs to adjust the potential bias in the recruitment of the cases and controls. After the adjustment of all the co-variates, the association persisted, indicating that there was no recruitment bias and that resistant genotype frequencies between groups were not influenced by ancestry. The rs12979860 has been the most important polymorphism in the region (Eslam et al., 2017). When, we arranged the haplotypes, including this SNP, our analysis showed that C-C combination at rs8109886 and rs12979860 demonstrated that the likelihood of abnormal CZS was reduced 14.3 times (OR = 0.07). Further, the genotypic combinations confirmed that CA/CC-CC (rs8109886-rs12979860) were strongly protective, while 93% of the mothers did not have CZS. In the same analysis on the fetuses, the results did not suggest any association between the *IFNL* SNP genotypes and the outcome, despite an OR value indicative of protection in rs8109886 CA/CC individuals.

Following previous clinical studies (Brasil et al., 2016), in our cohort, the determination of the trimester of pregnancy in which ZIKV infection occurs was a strong predictor factor for CZS outcome. Our findings demonstrated that maternal rs8109886 and rs12979860 genotypes should also be considered as a critical variable for abnormal CZS outcomes prediction (Figure 5). Despite the sample size, which is a limitation that increases uncertainty, it is remarkable that the absence of CZS outcome in mothers that carry the protection-associated genotype combination CC/CA – CC (rs8109886- rs12979860) considering ZIKV infection in all trimesters of pregnancy in our cohort where the genetic effect is even stronger in the second and third trimester of pregnancy. There was only one

fatal case of CZS in a CC/CA – CC mother that developed Zika symptoms in second trimester of pregnancy, characterized by hydrocephalus and arthrogryposis.

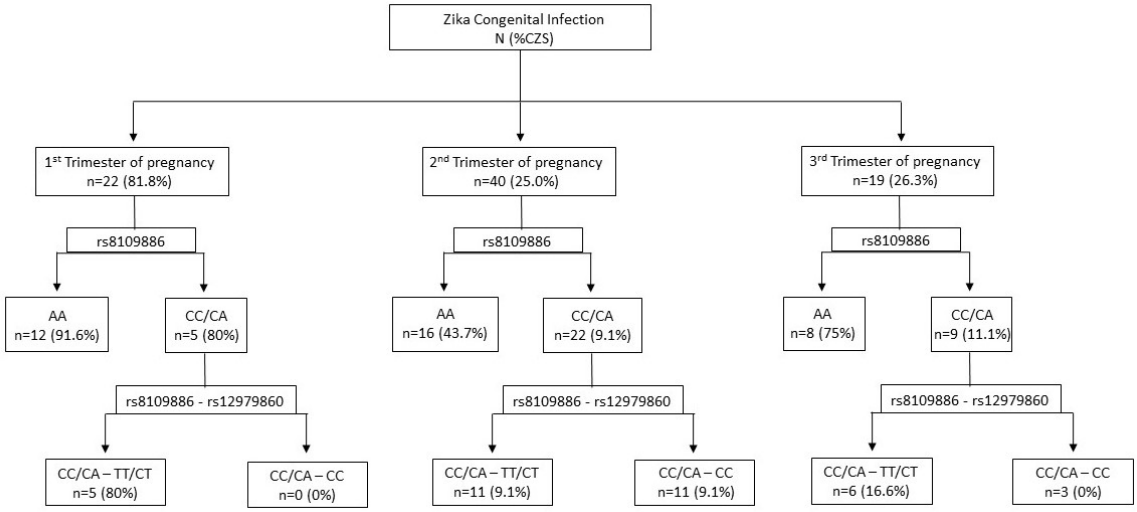

Figure 5. Event-based flowchart of CZS protection. The trimester of pregnancy which occurs first Zika symptoms and maternal genotypes of SNPs rs8109886 and rs12979860 was used as independent variables to determine the association with CZS outcome. The protection-associated tag genotypic combination (CC/AA – CC) (n=13) is absent in CZS cases independent of time of pregnancy which occurs zika symptoms. Concerning the infections in the first trimester of pregnancy, we found that irrespective of the rs8109886 and rs12979860 genotypes, 80% or more of the cases developed CZS, in contrast with second and third trimesters. Considering only rs8109886, this background seems to be associated with protection only for second and third trimester. For the second trimester, the frequency of CZS was almost five times higher among rs8109886 AA mothers. For the third trimester, genetic influence seems to be stronger since data shows 75% of CZS in AA against 11% in CC-CA mothers.

IFNL1-4 is mostly expressed by epithelial, plasmocytoid dendritic cells and macrophages (Kotenko and Durbin, 2017; Lazear et al., 2015), which are cell types presented in placenta. In this sense, our data show that the presence of inflammatory cells in deciduous strongly elicit the *IFNL1-4* expression in ZIKV-infected placenta. Notably, placenta from the abnormal CZS cases is associated with an impaired *IFNL2* response, accompanied by an uncontrolled and exacerbated Type-I IFN responses; particularly with an increased expression of *IFIT5*, parallel to a decrease in *ISG15* mRNA, which was already identified as being protective of ZIKV ocular manifestations (Singh et al., 2017). This profile of augmented type I IFN associated with severity is corroborated in ZIKV infected mice model (Yockey et al., 2018) and in other congenital TORCH infections (Racicot et al., 2017; Scott

et al., 2012). In addition, these mothers also had a low Type-I IFN response that characterizes protection; however, it is noteworthy that the studies that involved mice models demonstrated a lack of Type-I IFN response, also leading to CSZ (Miner et al., 2016; Yockey et al., 2018). Hence, we can hypothesize that a balanced production of Type-I IFN is genetically controlled by higher Type-III IFNs levels; this could, in turn, provide a proper protective response to ZIKV infection in the placenta, which could prevent CZS severe outcomes. Nevertheless, either genetic or functional findings should be independently replicated in other populations.

The PCR ZIKV+ placenta showed increased *TLR3* and *TLR8* mRNA expressions, which contribute as pattern recognition receptors for ZIKV uptake (Dang et al., 2016; Hamel et al., 2015; Luo et al., 2018; Tiwari et al., 2017). Although *in vitro* studies strongly suggest that *TYRO3* is the main entry receptor for ZIKV (Bagasra et al., 2017; Hamel et al., 2015), persistent ZIKV-infected placentas showed a decreased expression of *TYRO3* in PCR+ ZIKV individuals, corroborating recent findings in mice indicating that in complex organisms these receptors do not appear to be required for ZIKV infection (Hastings et al., 2017). Otherwise, increased expressions of *CLEC5A* and *DC-SIGN* could also suggest alternative routes for virus uptake or antiviral cellular response, as reported for other flavivirus infections (Chen et al., 2008, 2012; Smit et al., 2011; Tassaneetrithep et al., 2003). A higher expression of *BCL2*, *CARD9*, and *NRPL3* suggests that ZIKV could lead to apoptosis and activation of inflammasomes in placental cells (Huang et al., 2016; Khaiboullina et al., 2017; Miner et al., 2016; Tricarico et al., 2017).

In summary, our study showed a novel perspective to understand host-pathogen interaction during ZIKV infections in humans. During pregnancy, genetic regulatory pathways control tissue-specific *IFNL* expression during ZIKV congenital infection influencing fetal neurological damage. This novel pathway can help a better application of *IFNL*s responses toward custom pharmacological interventions to modulate its levels, which would likely affect and disrupt CNS development. In addition, the key role of rs8109886 SNP indicates that ZIKV and other TORCH infections could be evaluated concerning the host-directed therapies and medical follow-up during prenatal care.

Acknowledgements

The authors would like to thank Ms. Natália Pedra Gonçalves and Dr. Erica Louro da Fonseca from Vice Diretoria de Qualidade, Biomanguinhos, Fiocruz, for their help with ancestry analysis. We would also like to thank the team of Laboratório de Tecnologia

Imunológica, Vice Diretoria de Desenvolvimento de Biomanguinhos, Fiocruz, for their technical and management support. This work was supported by Biomanguinhos and Instituto Oswaldo Cruz, Fiocruz, Brazil.

Author Contributions

Conceptualization: MOM, ZV, PCCN, and TA; Data curation: TA, DPC, EAP, LCG, LG, MELM, and ZV; Formal analysis: TA, FK, AMVS, CCC, MRA, TLC, OCL, FSNM, LPF, and EFC. Investigation: AMVS, CB, JS, AFS. Funding acquisition and Resources: MM and MOM. Supervision: PCCN, ZV and MOM; Writing – original draft: TA; Writing – review & editing: DPC, PCCN, ZV, and MOM.

Competing interests

The authors declare no competing interests.

Data availability

The data that support the findings of this study are available from the corresponding author upon reasonable request.

EXPERIMENTAL PROCEDURES

Human subjects and sample collection. Our studies made use of the ongoing prospective clinical cohort study of ZIKV+ pregnant women and their infants at Children and Mothers Hospital (Instituto Fernandes Figueira, IFF/Fiocruz) in Rio de Janeiro, Brazil (IRB/CAAE: 52675616.0.000.5269). In this cohort, pregnant women who were ZIKV+ received their prenatal care at IFF/Fiocruz. Since December 2015, a total of 301 mothers who were suspected to have been infected by ZIKV during gestation were referred to IFF—a major public reference hospital in Rio de Janeiro for congenital infections and malformations. From this cohort study, 68 mothers (22.6%) were not confirmed to be ZIKV by RT-PCR; however, their infants displayed features that could be used to classify them as suffering from CZS(Moore et al., 2017). Among the 233 confirmed cases, 102 (43.8%) infants were considered symptomatic, presenting CNS and/or eye abnormalities at birth. CNS abnormalities include microcephaly, ventriculomegaly, cerebral calcifications, posterior fossa abnormalities, pachygyria, and lissencephaly, which were not mutually exclusive. Eye abnormalities included optic nerve atrophy, chorioretinal atrophy, pigment mottling, and hemorrhage which occurs frequently and is associated with CNS alterations. From those cases, 84 placentas (74 from congenital ZIKV infections and 10 uninfected) were accessed, processed, and analyzed for gene expression. Samples from mothers were tested for HIV, evidence of past DENV infection (by DENV IgG and IgM), and Chikungunya virus (CHIKV) (blood PCR). Maternal demographic, medical/prenatal history, and clinical findings were entered into case-report forms. All the infants underwent routine clinical and extensive neurologic evaluation at the time of birth; they were also tested for ZIKV vertical transmission (by PCR of infant blood and urine specimens), CHIKV infection (blood PCR), and syphilis and TORCH infections (toxoplasmosis, rubella, CMV, and herpes simplex virus; as determined by standard testing). The infants were evaluated for the following adverse neurologic outcomes: (a) microcephaly (head- circumference z score of less than -2), (b) abnormal brain imaging by pre- or post-natal ultrasound (e.g., computed tomography and/or magnetic resonance imaging), and/or (c) abnormal clinical examination (including neurologic, ocular, and/or auditory with abnormalities confirmed by a multidisciplinary team of neonatologists, neurologists, infectious disease specialists, geneticists, ophthalmologists, and physical therapists). From this cohort, adverse clinical outcomes (mostly neurologic) have been reported at birth in 46% of infants, and they have been found in infants born to mothers infected during all trimesters. Our study included ZIKV+ pregnant adult women >

18 years of age and their infants. The exclusion criteria were maternal HIV infection and pregnancies complicated by other congenital infections, known to cause infant neurologic damage (e.g., TORCH, CHIKV). Placental samples were collected at the time of delivery and were formalin-fixed, paraffin-embedded (FFPE), and stored in RNA later for posterior RNA extraction. For DNA analysis, pregnant women have 5 mL of blood collected at study enrollment, and for the newborns, an oral swab was collected.

Genetic studies: SNP selection and linkage disequilibrium analysis. The candidate SNPs selection for case-control association study was performed by integrating different tools: Principal Components Analysis (PCA), ANNOVAR (Wang et al., 2010), alelle frequencies, literature and HAPLOVIEW (Barrett et al., 2005). First, all SNPs located in the *IFNL* region (chr19:39,733,272-39,736,609-GRCh37/hg19) were recovered from African (ENS, GWD, LWK, MSL, and YRI) and European (CEU, FIN, GBR, IBS, and TSI) populations from 1000 Genomes Project phase 3 (The 1000 Genomes Project Consortium et al., 2015). Then, Principal Components Analysis (PCA) was performed using EIGENSOFT4.2 (Barrett et al., 2005). The use of this strategy in the functional SNPs selection assumes that, since the analyzed variability is of a functional genome region (it means, a gene), the clusters generated by PCA could be mainly influenced by the functionality. Thus, SNPs with high weight for Principal component 1 (PC1) could be a potential candidate for functional role. So, SNPs were sorted by decreasing the values of "SNP weight" for PC1, and the functional annotation of all the SNPs was performed using ANNOVAR (Wang et al., 2010), with refGene hg19 (11 Dez 2015). According to the functional category identified by ANNOVAR, the "SNP weight" for PC1 (with snpweight values among the higher 30, called top SNPs), minimal allele frequencies (MAF) in African and European populations (> 0.1), and associations with infectious diseases already reported in the literature, the SNPs present in the *IFNL* region were selected for genotyping and haplotype construction. Haplotypes inferences using the selected SNPs, haplotype frequencies, and linkage disequilibrium (LD) analysis for all the studied populations were performed using HAPLOVIEW (Barrett et al., 2005).

Genomic DNA extraction and SNP genotyping analysis. DNA extraction was performed from saliva swabs or whole blood cells collected from each individual newborn (n=129) and mother (n=92), respectively using the salting out method. After the extraction, the DNA was quantified in a Nanodrop ND 1000 spectrophotometer (Nanodrop Technologies). The

following polymorphisms were genotyped. SNPs for *IFNL*2-*IFNL*4: rs8099917 (C 11710096_10) located 8.9 kb upstream of the start codon of *IFNL*4 (T > G) and rs8109886 (C_11710100_10) located 3.3 kb upstream of the start codon of *IFNL*4 (A > C). *IFNL*4: rs12979860 (C_7820464_10) in intron 4 (C > T) and rs4803222 (C_7820457_10) in 5' UTR (C > G). All the SNPs were genotyped using the allelic discrimination method for real-time TaqMan assays (Applied Biosystems) in the ABI Prism 7000 Sequence Detection System or Step One Plus Real-time PCR System. About 50 ng of DNA was used in the genotyping reaction. Statistical analyses were performed using packages "snpassoc", "genetics" and "haplo.stats" in software R version 2.11.1, as previously described (2017a). Briefly, genotype frequencies were tested for Hardy– Weinberg equilibrium (HWE) using a Chi-square test. The genotypic, allelic, and carriers frequencies were calculated and compared in cases and controls by conditional logistic regression adjusted for ancestry and trimester of infection. Next, we compared the frequencies between CZS and no CZS separately. The values of linkage disequilibrium to SNPs studied in *IFNL* were estimated by r^2 and the haplotype frequencies were compared between cases and controls by logistic regression also adjusted for ancestry and trimester of infection. For mother-children SNP interaction, we used EMIM analysis using a multinomial model to test the existence (and estimate) of genotype relative risk parameters that may increase (or decrease) the possibility that a child is affected, as described previously(Howey and Cordell, 2012).

Ancestry analysis. Since Brazilian population is highly heterogeneous and ethnic classification is not uniformly defined, ancestry data is necessary to adjust the logistic regression and eliminate bias in the genetic associations(Barnholtz-Sloan et al., 2008). Thus, DNA samples were genotyped for 46 AIM-Indels in a multiplex PCR system followed by capillary electrophoresis in ABI 3500 Genetic Analyzer (Thermo Fisher), as described previously(Manta et al., 2013; Pereira et al., 2012). Allele calls were obtained by GeneMapper v.4.1 and results for individual and global ancestry estimates were performed by using the HGDP-CEPH diversity panel as reference (European, African and Native-american; K=3) in STRUCTURE v2.3. In the logistic regression performed in R, covariates AFR+EUR+AME or AFR+EUR were used to control for population stratification along with trimester of infection. Since both condition resulted in no differences in OR, we choose the EUR+AFR combination because they are the most predominant ancestry in the Brazilian population.

ZIKV PCR detection. RT-PCR was performed using the 2x QuantiTect Probe RT-PCR kit (Qiagen, Valencia, CA, USA) with the same primers and cycle times as previously

described(Lanciotti et al., 2008). All the assays were done in triplicates, and the fluorescence curves that crossed the threshold within or below 38 cycles were considered positive.

Gene expression profile analysis. Analysis of gene expression in placental tissue from pregnant mothers (control, with or without CZS samples) was performed using Fluidigm (Biomark platform) assays. Detailed data available under request. Our experimental design followed a workflow described previously(Guerreiro et al., 2013).

Real-time RT-PCR expression analysis. From routines created in R language for parsing raw foreground and background intensities, exported from the commercial platform Fluidigm®, we made the background correction and did the exploratory data analysis: fluorescence accumulation and melting curve graphs of Rn for each reaction in each gene. For the relative quantification of the expressions, the fluorescence accumulation data of each sample were used for fitting four parameters sigmoid curves using the library qPCR[56] for the R statistical package version 3.4.1(2017a). For each amplification, the cycle of quantification was determined as the maximum of the second derivative of the fit sigmoid curve and the efficiency, as the ratio between the fluorescence of the cycle of quantification and the fluorescence of the cycle that immediately preceded that. For each gene, the estimated efficiency was estimated by the mean of all the efficiencies for each amplification reaction of that gene. Endogenous controls used in normalization between the different amplified samples were selected by the geNorm method. Normalization factors were estimated for each sample using the geometric averaging of the selected normalized genes (Vandesompele et al., 2002).

Statistical analysis for gene expression. Pairwise comparisons of log-transformed (base 2) normalized expression means between/among groups of interest were performed by contrasts/differences (fold-changes), obtained after both bi- and multivariate linear models modified by ordinary least square regressions. Whenever the variable of interest had more than two levels, p-values were corrected by the Tukey Honest Significant Difference post-Hoc method(WS Cleveland, 1984). After all the gene-per-gene pairwise comparisons, we conducted a Type I error adjustment for multiple comparisons following the Holm-Bonferroni method(Holm, 1979). Different sets of confounding variables were selected by clinical experts and included in the multivariate models to adjust the fit effects for different variables of interest for all the genes. For the analysis, two-tailed levels of significance ≤

0.01, 0.05, and 0.1 were considered as “highly significant,” “significant,” and “suggestive,” respectively.

References

Adhikari, E.H., Nelson, D.B., Johnson, K.A., Jacobs, S., Rogers, V.L., Roberts, S.W., Sexton, T., McIntire, D.D., and Casey, B.M. (2017). Infant outcomes among women with Zika virus infection during pregnancy: results of a large prenatal Zika screening program. Am. J. Obstet. Gynecol. *216*, 292.e1-292.e8.

de Araújo, T.V.B., Ximenes, R.A. de A., Miranda-Filho, D. de B., Souza, W.V., Montarroyos, U.R., de Melo, A.P.L., Valongueiro, S., de Albuquerque, M. de F.P.M., Braga, C., Filho, S.P.B., et al. (2018). Association between microcephaly, Zika virus infection, and other risk factors in Brazil: final report of a case-control study. Lancet Infect. Dis. *18*, 328–336.

Bagasra, O., Addanki, K.C., Goodwin, G.R., Hughes, B.W., Pandey, P., and McLean, E. (2017). Cellular Targets and Receptor of Sexual Transmission of Zika Virus. Appl. Immunohistochem. Mol. Morphol. AIMM *25*, 679–686.

Barnholtz-Sloan, J.S., McEvoy, B., Shriver, M.D., and Rebbeck, T.R. (2008). Ancestry estimation and correction for population stratification in molecular epidemiologic association studies. Cancer Epidemiol. Biomark. Prev. Publ. Am. Assoc. Cancer Res. Cosponsored Am. Soc. Prev. Oncol. *17*, 471–477.

Barrett, J.C., Fry, B., Maller, J., and Daly, M.J. (2005). Haploview: analysis and visualization of LD and haplotype maps. Bioinformatics *21*, 263–265.

Bayer, A., Lennemann, N.J., Ouyang, Y., Bramley, J.C., Morosky, S., Marques, E.T.D.A., Cherry, S., Sadovsky, Y., and Coyne, C.B. (2016). Type III Interferons Produced by Human Placental Trophoblasts Confer Protection against Zika Virus Infection. Cell Host Microbe *19*, 705–712.

Brasil, P., Pereira, J.P., Moreira, M.E., Ribeiro Nogueira, R.M., Damasceno, L., Wakimoto, M., Rabello, R.S., Valderramos, S.G., Halai, U.-A., Salles, T.S., et al. (2016). Zika Virus Infection in Pregnant Women in Rio de Janeiro. N. Engl. J. Med. *375*, 2321–2334.

Caires-Júnior, L.C., Goulart, E., Melo, U.S., Araujo, B.H.S., Alvizi, L., Soares-Schanoski, A., de Oliveira, D.F., Kobayashi, G.S., Griesi-Oliveira, K., Musso, C.M., et al. (2018). Discordant congenital Zika syndrome twins show differential in vitro viral susceptibility of neural progenitor cells. Nat. Commun. *9*, 475.

Chen, S.-T., Lin, Y.-L., Huang, M.-T., Wu, M.-F., Cheng, S.-C., Lei, H.-Y., Lee, C.-K., Chiou, T.-W., Wong, C.-H., and Hsieh, S.-L. (2008). CLEC5A is critical for dengue-virus-induced lethal disease. Nature *453*, 672–676.

Chen, S.-T., Liu, R.-S., Wu, M.-F., Lin, Y.-L., Chen, S.-Y., Tan, D.T.-W., Chou, T.-Y., Tsai, I.-S., Li, L., and Hsieh, S.-L. (2012). CLEC5A regulates Japanese encephalitis virus-induced neuroinflammation and lethality. PLoS Pathog. *8*, e1002655.

Coyne, C.B., and Lazear, H.M. (2016). Zika virus - reigniting the TORCH. Nat. Rev. Microbiol. *14*, 707–715.

Dang, J., Tiwari, S.K., Lichinchi, G., Qin, Y., Patil, V.S., Eroshkin, A.M., and Rana, T.M. (2016). Zika Virus Depletes Neural Progenitors in Human Cerebral Organoids through Activation of the Innate Immune Receptor TLR3. Cell Stem Cell *19*, 258–265.

Dekaban, A.S. (1968). Abnormalities in children exposed to x-radiation during various stages of gestation: tentative timetable of radiation injury to the human fetus. I. J. Nucl. Med. Off. Publ. Soc. Nucl. Med. *9*, 471–477.

Delorme-Axford, E., Donker, R.B., Mouillet, J.-F., Chu, T., Bayer, A., Ouyang, Y., Wang, T., Stolz, D.B., Sarkar, S.N., Morelli, A.E., et al. (2013). Human placental trophoblasts confer viral resistance to recipient cells. Proc. Natl. Acad. Sci. *110*, 12048–12053.

Eslam, M., McLeod, D., Kelaeng, K.S., Mangia, A., Berg, T., Thabet, K., Irving, W.L., Dore, G.J., Sheridan, D., Grønbæk, H., et al. (2017). IFN-λ3, not IFN-λ4, likely mediates IFNL3-IFNL4 haplotype-dependent hepatic inflammation and fibrosis. Nat. Genet. *49*, 795–800.

Grant, A., Ponia, S.S., Tripathi, S., Balasubramaniam, V., Miorin, L., Sourisseau, M., Schwarz, M.C., Sánchez-Seco, M.P., Evans, M.J., Best, S.M., et al. (2016). Zika Virus Targets Human STAT2 to Inhibit Type I Interferon Signaling. Cell Host Microbe *19*, 882–890.

Guerreiro, L.T.A., Robottom-Ferreira, A.B., Ribeiro-Alves, M., Toledo-Pinto, T.G., Rosa Brito, T., Rosa, P.S., Sandoval, F.G., Jardim, M.R., Antunes, S.G., Shannon, E.J., et al. (2013). Gene expression profiling specifies chemokine, mitochondrial and lipid metabolism signatures in leprosy. PloS One *8*, e64748.

Hadeed, A.J., and Siegel, S.R. (1989). Maternal cocaine use during pregnancy: effect on the newborn infant. Pediatrics *84*, 205–210.

Hamel, R., Dejarnac, O., Wichit, S., Ekchariyawat, P., Neyret, A., Luplertlop, N., Perera-Lecoin, M., Surasombatpattana, P., Talignani, L., Thomas, F., et al. (2015). Biology of Zika Virus Infection in Human Skin Cells. J. Virol. *89*, 8880–8896.

Hastings, A.K., Yockey, L.J., Jagger, B.W., Hwang, J., Uraki, R., Gaitsch, H.F., Parnell, L.A., Cao, B., Mysorekar, I.U., Rothlin, C.V., et al. (2017). TAM Receptors Are Not Required for Zika Virus Infection in Mice. Cell Rep. *19*, 558–568.

Hirsch, A.J., Roberts, V.H.J., Grigsby, P.L., Haese, N., Schabel, M.C., Wang, X., Lo, J.O., Liu, Z., Kroenke, C.D., Smith, J.L., et al. (2018). Zika virus infection in pregnant rhesus macaques causes placental dysfunction and immunopathology. Nat. Commun. *9*.

Holm (1979). A Simple Sequentially Rejective Multiple Test Procedure. Vol. 6, No. 2, pp. 65–70.

Howey, R., and Cordell, H.J. (2012). PREMIM and EMIM: tools for estimation of maternal, imprinting and interaction effects using multinomial modelling. BMC Bioinformatics *13*, 149.

Huang, W.-C., Abraham, R., Shim, B.-S., Choe, H., and Page, D.T. (2016). Zika virus infection during the period of maximal brain growth causes microcephaly and corticospinal neuron apoptosis in wild type mice. Sci. Rep. *6*, 34793.

Jürgens, I., and Rey, A. (2018). Ocular findings in patients with microcephaly can suggest presumed congenital zika virus infection. Acta Ophthalmol. (Copenh.) *96*, 423–424.

Khaiboullina, S.F., Uppal, T., Sarkar, R., Gorzalski, A., St Jeor, S., and Verma, S.C. (2017). ZIKV infection regulates inflammasomes pathway for replication in monocytes. Sci. Rep. *7*, 16050.

Kotenko, S.V., and Durbin, J.E. (2017). Contribution of type III interferons to antiviral immunity: location, location, location. J. Biol. Chem. *292*, 7295–7303.

Lanciotti, R.S., Kosoy, O.L., Laven, J.J., Velez, J.O., Lambert, A.J., Johnson, A.J., Stanfield, S.M., and Duffy, M.R. (2008). Genetic and serologic properties of Zika virus associated with an epidemic, Yap State, Micronesia, 2007. Emerg. Infect. Dis. *14*, 1232–1239.

Lazear, H.M., Nice, T.J., and Diamond, M.S. (2015). Interferon-λ: Immune Functions at Barrier Surfaces and Beyond. Immunity *43*, 15–28.

Leviton, A., Kuban, K., Allred, E.N., Hecht, J.L., Onderdonk, A., O'Shea, T.M., McElrath, T., Paneth, N., and ELGAN Study Investigators (2010). Antenatal antecedents of a small head circumference at age 24-months post-term equivalent in a sample of infants born before the 28th post-menstrual week. Early Hum. Dev. *86*, 515–521.

Luo, H., Winkelmann, E.R., Fernandez-Salas, I., Li, L., Mayer, S.V., Danis-Lozano, R., Sanchez-Casas, R.M., Vasilakis, N., Tesh, R., Barrett, A.D., et al. (2018). Zika, dengue and yellow fever viruses induce differential anti-viral immune responses in human monocytic and first trimester trophoblast cells. Antiviral Res. *151*, 55–62.

Manta, F.S.N., Pereira, R., Caiafa, A., Silva, D.A., Gusmão, L., and Carvalho, E.F. (2013). Analysis of genetic ancestry in the admixed Brazilian population from Rio de Janeiro using 46 autosomal ancestry-informative indel markers. Ann. Hum. Biol. *40*, 94–98.

Miner, J.J., Cao, B., Govero, J., Smith, A.M., Fernandez, E., Cabrera, O.H., Garber, C., Noll, M., Klein, R.S., Noguchi, K.K., et al. (2016). Zika Virus Infection during Pregnancy in Mice Causes Placental Damage and Fetal Demise. Cell *165*, 1081–1091.

Moore, C.A., Staples, J.E., Dobyns, W.B., Pessoa, A., Ventura, C.V., Fonseca, E.B. da, Ribeiro, E.M., Ventura, L.O., Neto, N.N., Arena, J.F., et al. (2017). Characterizing the Pattern of Anomalies in Congenital Zika Syndrome for Pediatric Clinicians. JAMA Pediatr. *171*, 288–295.

Mostoufi-zadeh, M., Driscoll, S.G., Biano, S.A., and Kundsin, R.B. (1984). Placental evidence of cytomegalovirus infection of the fetus and neonate. Arch. Pathol. Lab. Med. *108*, 403–406.

Noronha, L. de, Zanluca, C., Azevedo, M.L.V., Luz, K.G., and Santos, C.N.D. dos (2016). Zika virus damages the human placental barrier and presents marked fetal neurotropism. Mem. Inst. Oswaldo Cruz *111*, 287–293.

O'Brien, T.R., Prokunina-Olsson, L., and Donnelly, R.P. (2014). IFN-λ4: the paradoxical new member of the interferon lambda family. J. Interferon Cytokine Res. Off. J. Int. Soc. Interferon Cytokine Res. *34*, 829–838.

Pereira, R., Phillips, C., Pinto, N., Santos, C., dos Santos, S.E.B., Amorim, A., Carracedo, Á., and Gusmão, L. (2012). Straightforward inference of ancestry and admixture proportions through ancestry-informative insertion deletion multiplexing. PloS One *7*, e29684.

Price, A.A., Tedesco, D., Prasad, M.R., Workowski, K.A., Walker, C.M., Suthar, M.S., Honegger, J.R., and Grakoui, A. (2016). Prolonged activation of innate antiviral gene signature after childbirth is determined by IFNL3 genotype. Proc. Natl. Acad. Sci. U. S. A. *113*, 10678–10683.

Price, A.L., Patterson, N.J., Plenge, R.M., Weinblatt, M.E., Shadick, N.A., and Reich, D. (2006). Principal components analysis corrects for stratification in genome-wide association studies. Nat. Genet. *38*, 904–909.

Quicke, K.M., Bowen, J.R., Johnson, E.L., McDonald, C.E., Ma, H., O'Neal, J.T., Rajakumar, A., Wrammert, J., Rimawi, B.H., Pulendran, B., et al. (2016). Zika Virus Infects Human Placental Macrophages. Cell Host Microbe *20*, 83–90.

Racicot, K., Aldo, P., El-Guindy, A., Kwon, J.-Y., Romero, R., and Mor, G. (2017). Cutting Edge: Fetal/Placental Type I IFN Can Affect Maternal Survival and Fetal Viral Load during Viral Infection. J. Immunol. Baltim. Md 1950 *198*, 3029–3032.

Relich, R.F., and Loeffelholz, M. (2017). Zika Virus. Clin. Lab. Med. *37*, 253–267.

Ritz, C., and Spiess, A.-N. (2008). qpcR: an R package for sigmoidal model selection in quantitative real-time polymerase chain reaction analysis. Bioinforma. Oxf. Engl. *24*, 1549–1551.

Sarkar, M., Aouzierat, B., Bacchetti, P., Prokunina-Olsson, L., French, A., Seaberg, E., O'Brien, T.R., Kuniholm, M.H., Minkoff, H., Plankey, M., et al. (2015). Association of IFNL3 and IFNL4 polymorphisms with liver-related mortality in a multiracial cohort of HIV/HCV-coinfected women. J. Viral Hepat. *22*, 1055–1060.

Scott, G.M., Chow, S.S.W., Craig, M.E., Pang, C.N.I., Hall, B., Wilkins, M.R., Jones, C.A., Lloyd, A.R., and Rawlinson, W.D. (2012). Cytomegalovirus Infection During Pregnancy With Maternofetal Transmission Induces a Proinflammatory Cytokine Bias in Placenta and Amniotic Fluid. J. Infect. Dis. *205*, 1305–1310.

Singh, P.K., Guest, J.-M., Kanwar, M., Boss, J., Gao, N., Juzych, M.S., Abrams, G.W., Yu, F.-S., and Kumar, A. (2017). Zika virus infects cells lining the blood-retinal barrier and causes chorioretinal atrophy in mouse eyes. JCI Insight *2*, e92340.

Smit, J.M., Moesker, B., Rodenhuis-Zybert, I., and Wilschut, J. (2011). Flavivirus cell entry and membrane fusion. Viruses *3*, 160–171.

Suppiah, V., Moldovan, M., Ahlenstiel, G., Berg, T., Weltman, M., Abate, M.L., Bassendine, M., Spengler, U., Dore, G.J., Powell, E., et al. (2009). IL28B is associated with response to chronic hepatitis C interferon-alpha and ribavirin therapy. Nat. Genet. *41*, 1100–1104.

Tabata, T., Petitt, M., Puerta-Guardo, H., Michlmayr, D., Wang, C., Fang-Hoover, J., Harris, E., and Pereira, L. (2016). Zika Virus Targets Different Primary Human Placental Cells, Suggesting Two Routes for Vertical Transmission. Cell Host Microbe *20*, 155–166.

Tanaka, Y., Nishida, N., Sugiyama, M., Kurosaki, M., Matsuura, K., Sakamoto, N., Nakagawa, M., Korenaga, M., Hino, K., Hige, S., et al. (2009). Genome-wide association of IL28B with response to pegylated interferon-alpha and ribavirin therapy for chronic hepatitis C. Nat. Genet. *41*, 1105–1109.

Tassaneetrithep, B., Burgess, T.H., Granelli-Piperno, A., Trumpfheller, C., Finke, J., Sun, W., Eller, M.A., Pattanapanyasat, K., Sarasombath, S., Birx, D.L., et al. (2003). DC-SIGN (CD209) mediates dengue virus infection of human dendritic cells. J. Exp. Med. *197*, 823–829.

The 1000 Genomes Project Consortium, Sudmant, P.H., Rausch, T., Gardner, E.J., Handsaker, R.E., Abyzov, A., Huddleston, J., Zhang, Y., Ye, K., Jun, G., et al. (2015). An integrated map of structural variation in 2,504 human genomes. Nature *526*, 75–81.

Tiwari, S.K., Dang, J., Qin, Y., Lichinchi, G., Bansal, V., and Rana, T.M. (2017). Zika virus infection reprograms global transcription of host cells to allow sustained infection. Emerg. Microbes Infect. *6*, e24.

Tricarico, P.M., Caracciolo, I., Crovella, S., and D'Agaro, P. (2017). Zika virus induces inflammasome activation in the glial cell line U87-MG. Biochem. Biophys. Res. Commun. *492*, 597–602.

Vandesompele, J., De Preter, K., Pattyn, F., Poppe, B., Van Roy, N., De Paepe, A., and Speleman, F. (2002). Accurate normalization of real-time quantitative RT-PCR data by geometric averaging of multiple internal control genes. Genome Biol. *3*, RESEARCH0034.

Wang, K., Li, M., and Hakonarson, H. (2010). ANNOVAR: functional annotation of genetic variants from high-throughput sequencing data. Nucleic Acids Res. *38*, e164–e164.

Weisblum, Y., Oiknine-Djian, E., Vorontsov, O.M., Haimov-Kochman, R., Zakay-Rones, Z., Meir, K., Shveiky, D., Elgavish, S., Nevo, Y., Roseman, M., et al. (2017). Zika Virus Infects Early- and Midgestation Human Maternal Decidual Tissues, Inducing Distinct Innate Tissue Responses in the Maternal-Fetal Interface. J. Virol. *91*.

Wen, Z., Song, H., and Ming, G.-L. (2017). How does Zika virus cause microcephaly? Genes Dev. *31*, 849–861.

WS Cleveland, J.T. (1984). The collected works of John W. Tukey.

Yockey, L.J., Jurado, K.A., Arora, N., Millet, A., Rakib, T., Milano, K.M., Hastings, A.K., Fikrig, E., Kong, Y., Horvath, T.L., et al. (2018). Type I interferons instigate fetal demise after Zika virus infection. Sci. Immunol. *3*.

R Core Team (2017a). R: a language and environment for statistical computing.

World Health Organization (2017b). weekly epidemiological report.